Sensors and Actuators B 258 (2018) 163–171

Contents lists available at ScienceDirect

Sensors and Actuators B: Chemical

journal homepage: www.elsevier.com/locate/snb

SERS activated platform with three-dimensional hot spots and tunable nanometer gap

Chao Zhang[a,b,*,1], Chonghui Li[a,1], Jing Yu[a,b], Shouzhen Jiang[a,b], Shicai Xu[c], Cheng Yang[a,b], Yan Jun Liu[d], Xingguo Gao[e], Aihua Liu[a], Baoyuan Man[a,*]

[a] School of Physics and Electronics, Shandong Normal University, Jinan 250014, PR China
[b] Institute of Materials and Clean Energy, Shandong Normal University, Jinan 250014, PR China
[c] College of Physics and Electronic Information, Dezhou University, Dezhou 253023, PR China
[d] Department of Electrical and Electronic Engineering, Southern University of Science and Technology, Shenzhen 518055, PR China
[e] School of Science, Qilu University of Technology, Jinan 250353, PR China

ARTICLE INFO

Article history:
Received 17 April 2017
Received in revised form 17 October 2017
Accepted 17 November 2017
Available online 20 November 2017

Keywords:
AgNPs
graphene@AuNPs
SERS
Tunable nano gap
Malachite green

ABSTRACT

Hot spots have been considered as a dominant role in surface enhancement Raman scattering (SERS). Its generation cannot be separated from the ultra-small nanogaps, which will tremendously contribute to the strong electromagnetic field. We propose a AgNPs/graphene@AuNPs system with three-dimensional hot spots and tunable nanometer gap by changing the layer of graphene with a simple and facile method. The excellent SERS behaviors of the proposed AgNPs/graphene@AuNPs substrate are demonstrated experimentally using rhodamine 6G (R6G) and crystal violet (CV) as probe molecules and theoretically using commercial COMSOL software. The excellent SERS behaviors can be attributed to the electromagnetic mechanism (EM) in all three dimensions introduced by the lateral nanogaps (AgNP-AgNP) and the vertical nanogaps (AgNP-AuNPs), and the chemical enhancement mechanism (CM) induced by the graphene film. For practical application, the prepared sensitive AgNPs/graphene@AuNPs SERS substrate was used to detect Malachite green (MG) in sea water, which provides a bran-new avenue for the detection of biological and chemical molecule.

1. Introduction

Surface-enhanced Raman scattering (SERS), as a fascinating and powerful spectroscopy technique, can achieve the detection of low-concentration molecules by an enhancement factor up to 10^{14} or more [1–3]. Now, it has been widely accepted that the lateral nanogap in noble metal can effectively focus the incident light and restrict the light around the nanogap, which will excite the surface plasmon resonance and result in SERS enhancement based on electromagnetic mechanism (EM) [4–8]. To achieve the lateral nanogap-embedded structures, multifarious fabrication techniques have been presented and researched in recent years, such as lithography [9–11], shadow evaporation [12] and vapor transport method [13,14]. However, these fabrication techniques are challenging, expensive and time-consuming. What's more, it is a huge challenge to achieve the mass-production with excellent repeatability. Compared with these lateral nanogaps, the vertical nanogaps (such as Au single nanowire/Au film, [14] CuNPs/Cu film, [15] AuNPs/AuNPs, [16] AuNPs/AuNPs with a rippled structure [17] and AuNPs/Cu foil [18]) can be obtained by relatively simple and lost-cost technique. These studies have demonstrated that the highly localized field originated between the vertical nanogaps can introduce a further strong SERS enhancement. As the lower adsorption capacity of these metal nanogaps for some molecules and the signal variations of molecule-metal contact, it is hard to achieve ideal SERS substrates with well stability and reproducibility, which will limit their practical applications. It has been demonstrated that by introducing an ultrathin inert shell (such as TiO_2, [19] Fe_3O_4, [20] SiO_2 [21] or Al_2O_3 [22,23]) on the surface of the metal nanoparticles, one can improve the SERS behaviors of the metal nanogaps. But, in these technologies, the materials and thickness of coating shell, as the main roles, are challenging to be formed around the mintage metal (Ag, Au and Cu) core. In addition, some expensive precision instruments are required in the processes above. Therefore, it is greatly vital to find a nanomaterial as sub-nanospacer that can be easily integrated to SERS substrate.

* Corresponding authors at: School of Physics and Electronics and Institute of Materials and Clean Energy, Shandong Normal University, Jinan 250014, PR China.
E-mail addresses: czsdnu@126.com (C. Zhang), byman@sdnu.edu.cn (B. Man).
[1] These authors contributed equally.

https://doi.org/10.1016/j.snb.2017.11.080
0925-4005/

Graphene, as a typical 2-dimensional (2D) material, has been widely used in multifarious field by the virtue of its excellent properties and distinctive structure. [24–28] Recently, graphene, with the potential for improving the SERS enhancement through a chemical enhancement (CM) mechanism, has been of particular interest for researchers. Graphene as an outstanding candidate for SERS possesses the following attractive virtues: (1) the large specific surface area of graphene makes it as a perfect molecule enricher, which can control the molecular distribution and allow the molecular better contact with the SERS substrate [14]. (2) graphene can passivate the surface of metal nanoparticles and guarantee the chemical stability of the SERS substrate [29]. (3) graphene with its intrinsic single-atom structure allows it sever as an excellent sub-nm spacer and create a uniform nanogap between metal nanoparticles [15]. These excellent advantages equip graphene as an outstanding alternative SERS substrate for achieving high-sensitivity, well-stability, homogeneous and reliable SERS signals.

Inspired by their advantages, we combine the AuNPs, AgNPs and graphene and form the construction of AgNPs/graphene@AuNPs with a simple and facile method attempting to obtain the sensitive, stable, homogeneous and reproducible SERS behaviors. The excellent surface-enhanced Raman scattering (SERS) behaviors of the proposed AgNPs/graphene@AuNPs substrate are demonstrated experimentally using rhodamine 6G (R6G) and crystal violet (CV) as probe molecules and theoretically using commercial COMSOL software. Here, the prominent SERS behaviors can be attributed to the EM introduced by the lateral nanogaps (AgNP-AgNP) and the vertical nanogaps (AgNP-AuNPs), and the CM induced by the graphene film. In the proposed AgNPs/graphene@AuNPs substrate, the surface plasmon resonance in all three dimensions can be effectively excited by the lateral and vertical nanogaps, which is much beneficial for the enhancement of the EM. Besides, the graphene not only can provide the SERS enhancement from CM, but also can act as a nanometer ruler to accurately control the size of the nanogaps by changing the layers of graphene, which will promote to better investigate the role of the nanogaps. Malachite green (MG), as a harmful carcinogen, has been frequently and illegally abused in aquaculture to breed the aquatic during the past centenary. The residual of the MG oxalate in the aquatic animal can induce the teratogenesis and mutation of the organs in human beings, which will further result in the canceration of the organs such as liver, heart, kidney and so on. Hence, many countries have taken measures to control the abuse of the MG and keep it out of the food. Therefore, it is urgent need to develop a highly sensitive method for the MG molecules detection. On the basis of the AgNPs/graphene@AuNPs, we achieved the low limit (as low as the European Union's standard: 5.48 nM) of detection of the MG in deionized (DI) water and sea water by SERS. We expect that this sensitive and high-efficiency SERS substrate can open a bran-new avenue for the detection of biological and chemical molecule.

2. Experimental sections

2.1. Fabrications of the AgNPs/graphene@AuNPs, graphene@AuNPs and AgNPs/graphene substrates

The SiO_2 substrates were cleaned according to our previous report [30]. The uniform Au (Au wires of 0.0020 g were used) film was evaporated on the SiO_2 substrates by physical vapor deposition (PVD). After this process, monolayer graphene fabricated by the CVD method was transferred on the SiO_2 substrate as the following step: polymethyl methacrylate (PMMA), which is a support and protective layer, was coated on graphene on Cu foil. And then the derived sample was immersed into $FeCl_3$ solution (~1 M) to absolutely etch Cu foil. After that the remaining PMMA/graphene layer was carefully transferred into DI water for 5 times to remove the residual etching solution. Next, PMMA/graphene layer in DI water was gently fished up by the SiO_2 substrate and was blown dry under nitrogen atmosphere followed by baking under 130 °C to make PMMA/graphene layer closely paste on the surface of SiO_2. After that the sample was put into 100 mL acetone solution and heated to 80 °C for 10 times to completely remove the coating layer (PMMA). After that, uniform Ag (Ag wires of 0.0030 g were used) film was evaporated on the sample by PVD. Finally, all obtained samples were put into the tube furnace (OTL1200 bought from Nanjing NanDa Instrument Plant) and annealed at 500 °C for 30 min in the 40 sccm Ar environment to respectively dewet the Au film and Ag film into the AuNPs and AgNPs. The graphene@AuNPs and AgNPs/graphene substrate were fabricated using the similar method.

2.2. Apparatus and characterization

To clearly observe the surface morphology of the above mentioned samples, atomic force microscope (AFM Bruker Multimode 8), scanning electron microscope (SEM ZEISS Gemini SUPRA55) with the energy dispersive spectrometer (EDS) and transmission electron microscope (TEM JEM-2100) were carried out. UV-vis Spectrophotometer (UV-4501S, Tianjin Gangdong Sci. & Tech. development CO., LTD) was performed to analyze the optical characterization of these samples.

2.3. SERS spectra measurements

SERS spectra were detected by Raman spectrometer (Horiba HR Evolution 800) with laser wavelength of 532 nm. The laser excitation energy and spot respectively were respectively 0.48 mW and 1 μm. Throughout the experiment, the diffraction grid was set as 600 gr/mm and the integration time was set as 8 s.

3. Results and discussion

Fig. 1 schematically illustrates the process for the fabrication of the proposed AgNPs/graphene@AuNPs which is described in detail in the methods. A 7 nm thick Au film as exhibited in Fig. S1(a) was deposited on the SiO_2 substrate with a thermal evaporation method followed by the double transfer of the graphene to form the bilayer graphene/Au film. Subsequently, a 16 nm thick Ag film as shown in Fig. S1(b) was deposited on the graphene/Au film with a thermal evaporation method and annealed at 500 °Cfor 30 min in the Ar environment to respectively dewet the Au film and Ag film into the AuNPs and AgNPs. The nanometer gap between the AuNPs and AgNPs can be simply controlled and tuned by changing the transfer time for the graphene.

Scanning electron microscopy (SEM) was carried out to investigate the surface morphology of the prepared AgNPs/graphene@AuNPs. The low-magnification image showed in Fig. 2(a) exhibits that the SiO_2 substrate is covered by a large amount of well-ordered and uniform nanoparticles after the annealing process, which indicates that the Au film and Ag film respectively dewet to AuNPs and AgNPs and enables the AgNPs/graphene@AuNPs substrate possessing high-density and uniform hotpots for the SERS. In order to give strong support for the well distribution of these nanoparticles and identify the size, we further perform the SEM measurement under a larger magnification (Fig. 2(b)), where layered nanoparticles are observed. Combined with the energy dispersive spectrometer (EDS) map shown in Fig. S2, we can identify that the bottom and small nanoparticles are AuNPs and the top and large nanoparticles are AgNPs. The diameter and diameter distribution of these nanoparticles shown in Fig. 2(b) are summarized in Figs. 2(c), (d) and S3

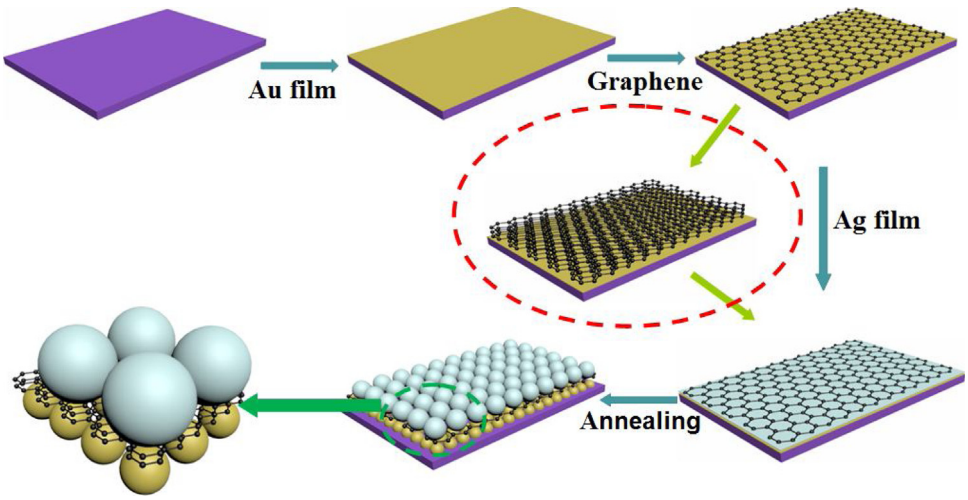

Fig. 1. Schematic illustration of the fabrication of the proposed AgNPs/graphene@AuNPs.

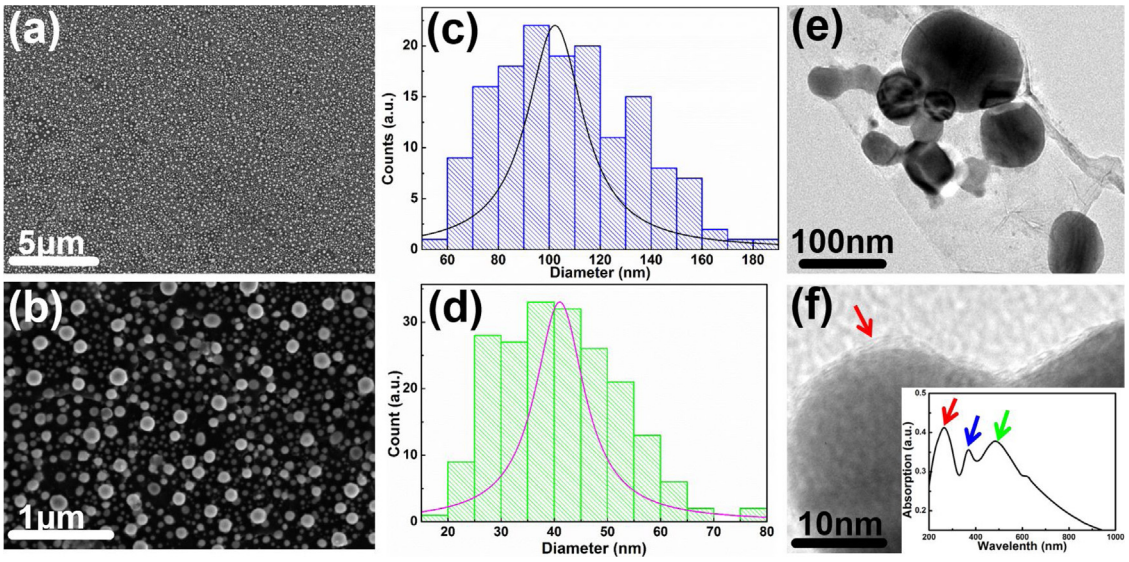

Fig. 2. (a) and (b) SEM images of the AgNPs/graphene@AuNPs under different magnification. (c) and (d) Diameter distribution of the AgNPs and AuNPs. (e) TEM image of the AgNPs/graphene. (f) TEM image of the graphene@AuNPs (insert: the absorption spectrum of the AgNPs/graphene@AuNPs).

with the help of the software Nano measurer. The diameters of the AgNPs and AuNPs both have a weak fluctuation as shown in Fig. S3. Just as the histograms exhibited in Fig. 2(c) and (d), the diameter distributions of the AgNPs and AuNPs are all complied with a typical Gaussian curve. The peak positions of the AgNPs and AuNPs respectively center at ~100 nm and ~40 nm, which implies that the average diameters are respectively about 100 and 40 nm, respectively with a gap of 30 and 15 nm between nanoparticles. To provide a more visualized exhibition of the structure of the proposed AgNPs/graphene@AuNPs, the transmission electron microscope (TEM) measurement was implemented on the AgNPs/graphene@AuNPs completely liberated from the SiO_2 substrate. Just as expected in Fig. 2(e), AgNPs associated with are observed and the average diameter of the AgNPs is 100 nm, which is well consistent with the SEM results. In Fig. 2(f), typical graphene@AuNPs is presented, which can be attributed to the annealing process. Not only dewet the film to nanaparticles, the annealing process but also can improve the contact between the graphene and Au NPs and form the quasi core-shell structure [16], which is much beneficial for the high SERS sensitivity [8,29]. What's more, it is very interesting to note that three peaks can be detected in the absorption spectrum insert in Fig. 2(f). These peaks can be respectively assigned to the absorption of graphene, AgNPs and AuNPs, which provides us further credible evidence for the successful fabrication of the AgNPs/graphene@AuNPs and is well agreed with the EDS results.

e respectively choose the R6G and CV as probe molecule to evaluate the SERS activity of the proposed AgNPs/graphene@AuNPs substrate and all the Raman spectra were collected on the same conditions. We can detect the characteristic Raman peaks of R6G and CV for the concentration respectively from 10^{-5} to 10^{-11} M and from 10^{-5} to 10^{-12} M as well as the peaks of graphene. Besides, the typical Raman spectra can still be observed even with lower concentration of 10^{-11} and 10^{-12} M respectively for R6G and CV (Fig. S4), which demonstrates the high sensitivity of the proposed AgNPs/graphene@AuNPs substrate. The high sensitivity of the proposed AgNPs/graphene@AuNPs substrate can be attributed to the surface plasmon resonance in all three dimensions effectively excited by the lateral and vertical nanogaps. The enhancement factors of the AgNPs/graphene@AuNPs substrate will be further discussed in detail later. The primary vibrations of R6G and CV are confirmed according to the previous reports. [1,8,29] We can also

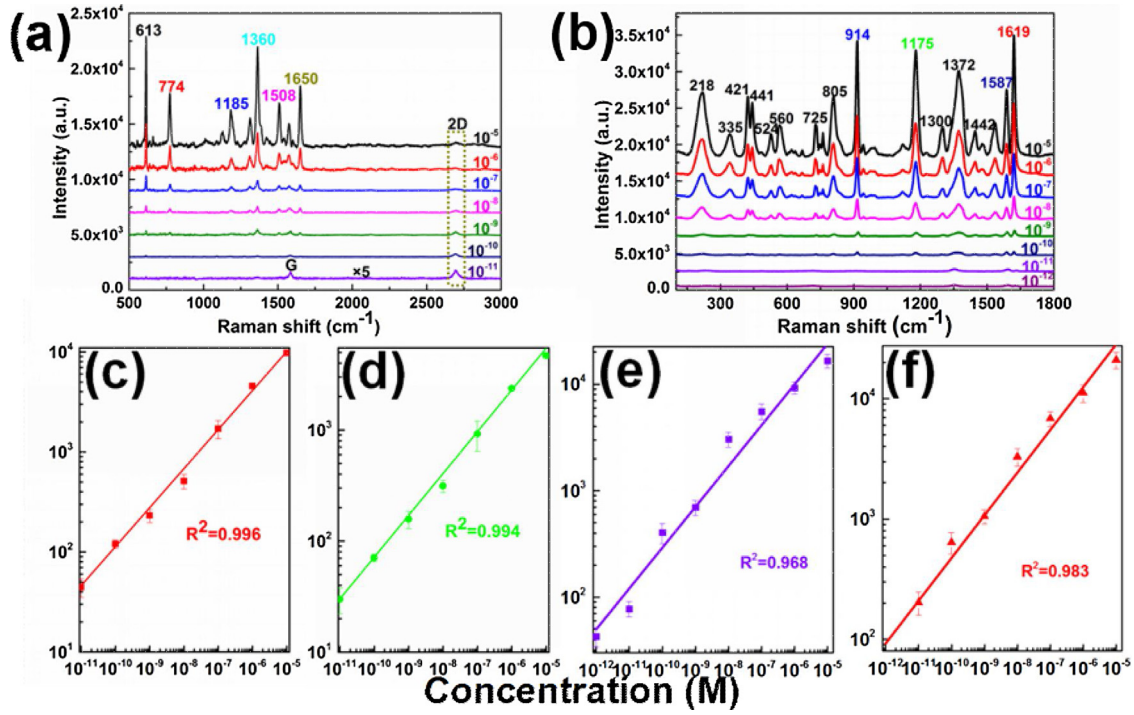

Fig. 3. (a) and (b) Raman spectra of R6G and CV on the AgNPs/graphene@AuNPs substrate respectively from 10^{-5} to 10^{-10} M and from 10^{-5} to 10^{-12} M. (c) and (d) Intensity of peaks at 613 and 774 cm^{-1} for R6G as a function of the molecular concentration. (e) and (f) Intensity of peaks at 914 and 1619 cm^{-1} for CV as a function of the molecular concentration.

observed in Fig. 3(a) and 3(b) that the intensities of the SERS signals for the R6G and CV molecular both gradually rise with the increase of the concentration, which indicates that the intensities of the characteristic Raman peaks are proportional to the numbers of molecules. To investigate the ability of this quantitative detection for molecules, the linear fit curves of the vibrations of R6G located at 613 and 774 cm^{-1} and the vibrations of CV located at 914 and 1619 cm^{-1} versus the concentrations are illustrated in Fig. 3(c)–(f). To ensure the dependability of the data, the average intensity based on ten spectra randomly collected on the proposed AgNPs/graphene@AuNPs substrate is chosen. It is thoroughly obvious that reasonable linear responses with the high coefficient of determination (R^2) for both R6G and CV molecular in log scale are achieved between the intensity of SERS signal and the concentration.

Besides the SERS activity and the ability of the quantitative detection, the homogeneity of the SERS signal and the reproducibility of the SERS substrate are the additional indispensable parameters for the practical application. Fig. 4(a) and (b) respectively present the SERS spectra of the R6G with a concentration of 10^{-5} M and CV with a concentration of 10^{-9} M randomly collected on AgNPs/graphene@AuNPs substrate from thirty points. Just as exhibited in Fig. 4(a), the SERS spectra of R6G with a concentration of 10^{-5} M are greatly well consistent between each other and the intensities for various peaks only fluctuate quite mildly. Similar phenomena are observed for the case of CV with a concentration of 10^{-9} M in Fig. 4(b) and the Raman detect of the proposed substrate in Fig. S5. The excellent conformity of the SERS spectra for both R6G and CV and the Raman spectra of the pure prepared substrate indicate the perfect homogeneity of the AgNPs/graphene@AuNPs substrate, which can be ascribed to the well-ordered and uniform AgNPs and AuNPs as well as the existence of the graphene. The well-ordered and uniform AgNPs and AuNPs is much beneficial for the acquisition of well distributed three-dimensional hot spots and the graphene can make the molecular well distributed around the three-dimensional hot spots further allowing the probe molecular contact well with the SERS substrate. Therefore, in our case we can achieve the SERS signals with high homogeneity. Fig. 4(c) and (d) respectively show the intensity distribution of the peak at 613 cm^{-1} for the R6G with a concentration of 10^{-5} M and 1619 cm^{-1} for the CV with a concentration of 10^{-7} M from 10 different batches of AgNPs/graphene@AuNPs substrates. The green line in Fig. 4(c) and (d) are the average intensities of the peak at 613 cm^{-1} for the R6G and 1619 cm^{-1} for the CV from these 10 different batches of AgNPs/graphene@AuNPs substrates. The individual intensity of these two representative peaks from the same batch is calculated based on ten spectra randomly collected on the AgNPs/graphene@AuNPs substrate. It is obvious that for both the case of R6G and CV, all the data exhibit a minor fluctuation around the average intensity and the variation ranges for R6G and CV are respectively confined in the region from −6.7% to +9.8% and from −8% to +9.1%. What's more, it should be noted that most of the ten data lie within ±6%, which is more superior to the requirements for practical SERS measurements (deviation should be within 20%) [31]. The prominent reproducibility of the proposed AgNPs/graphene@AuNPs substrate can be assigned to the following aspects: the facile reproduction of the AgNPs/graphene@AuNPs substrate can reduce the signal fluctuations induced by the substrate and the well-controlled graphene as a perfect molecule enricher can homogenously capture the probe molecules and effectively suppress the background fluorescence improving the reproducibility of the SERS substrate.

To further estimate the SERS activity of the proposed AgNPs/graphene@AuNPs substrate, the SERS spectra of R6G and CV with concentration of 10^{-5} M on the graphene@AuNPs and AgNPs/graphene are also collected in the same condition. For the cases of both graphene@AuNPs, AgNPs/graphene and AgNPs/graphene@AuNPs substrate, as shown in Fig. 5(a) and (b), all the typical Raman peaks of R6G and CV are observed in a sharp form, which indicates the excellent signal-to-noise ratio and can be attributed to the existence of graphene. It is distinct that the intensities of SERS spectra on the AgNPs/graphene@AuNPs are much

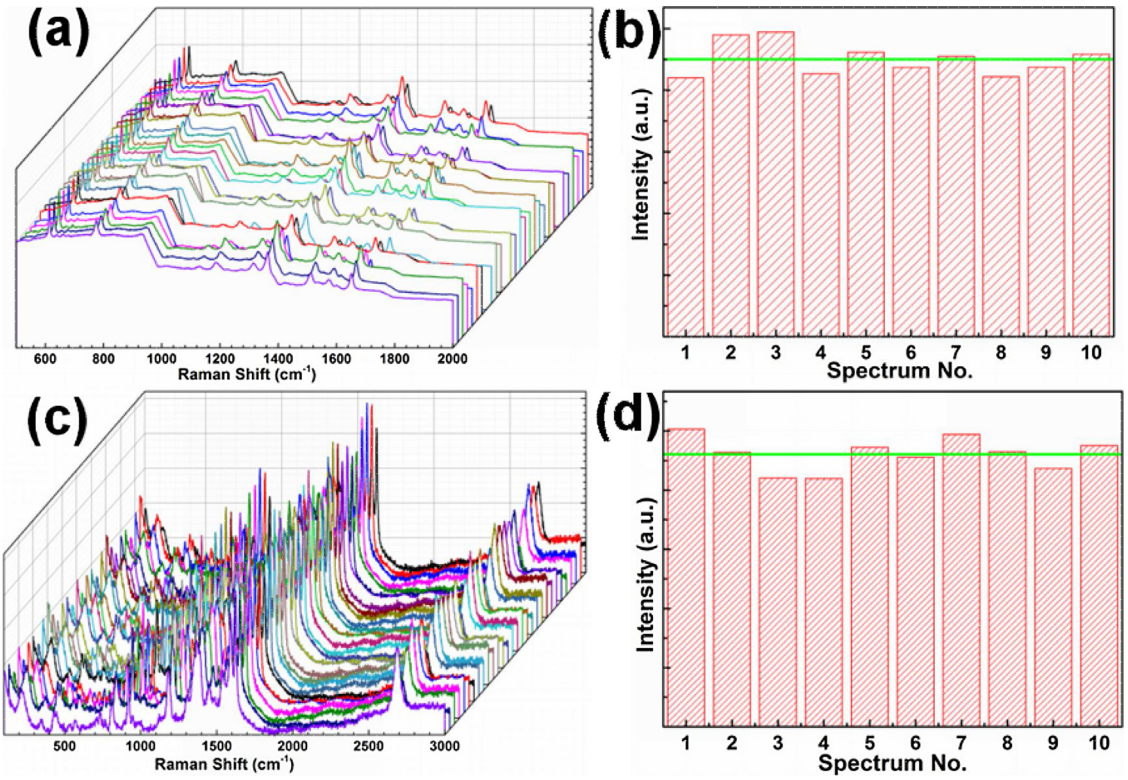

Fig. 4. (a) and (b) Raman spectra of R6G with a concentration of 10^{-5} M and CV with a concentration of 10^{-9} M randomly collected on the same AgNPs/graphene@AuNPs substrate. (c) and (d) Intensity distribution of the peak at 613 cm^{-1} for the R6G with a concentration of 10^{-5} M and 1619 cm^{-1} for the CV with a concentration of 10^{-7} M from 10 different batches of AgNPs/graphene@AuNPs substrates.

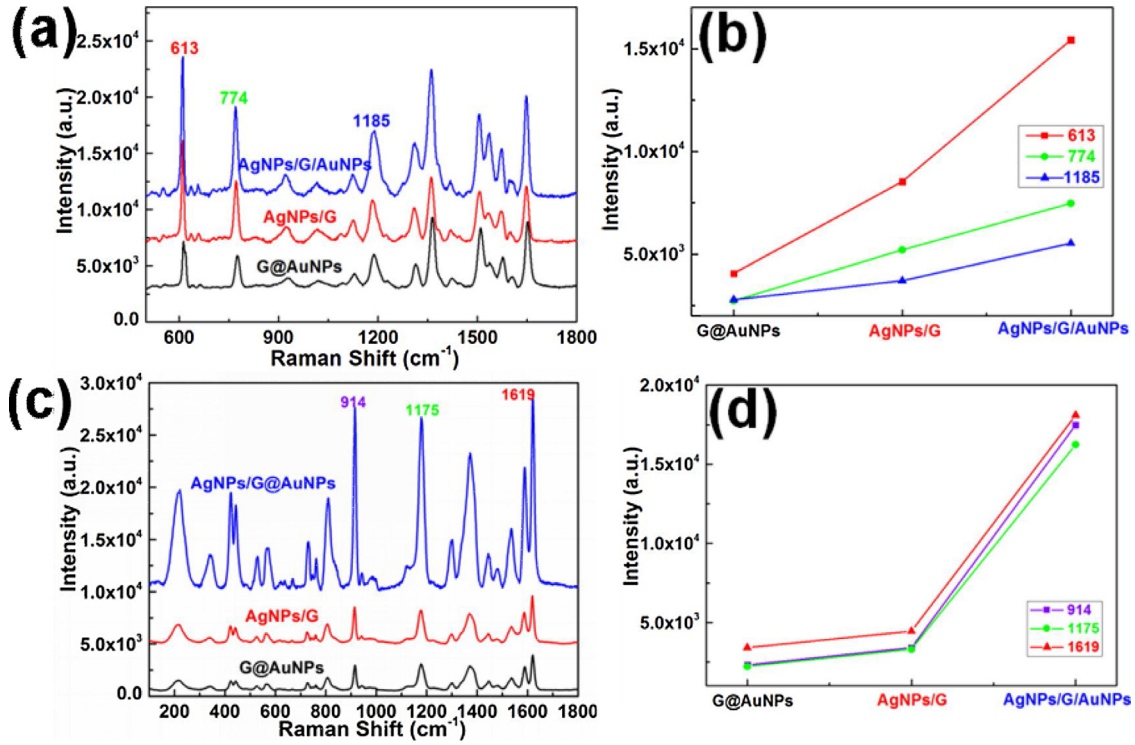

Fig. 5. (a) and (b) Raman spectra of R6G and CV with concentration of 10^{-5} M on the graphene@AuNPs, AgNPs/graphene and AgNPs/graphene@AuNPs substrate. (c) Intensity of the peak at 613, 774, 1185 cm^{-1} for R6G with concentration of 10^{-5} M. (d) Intensity of the peak at 914, 1175, 1619 cm^{-1} for CV with concentration of 10^{-5} M.

stronger than those on graphene@AuNPs and AgNPs/graphene. What's more, the intensities of SERS spectra on the AgNPs/graphene are similar with that on graphene@AuNPs and the former is little stronger than the latter. Fig. 5(c) and (d) respectively plot the intensity of the SERS signal at 613, 774, 1185 cm^{-1} for R6G and 914, 1175, 1619 cm^{-1} for CV. The peaks of R6G at 613, 774, 1185 cm^{-1} on the

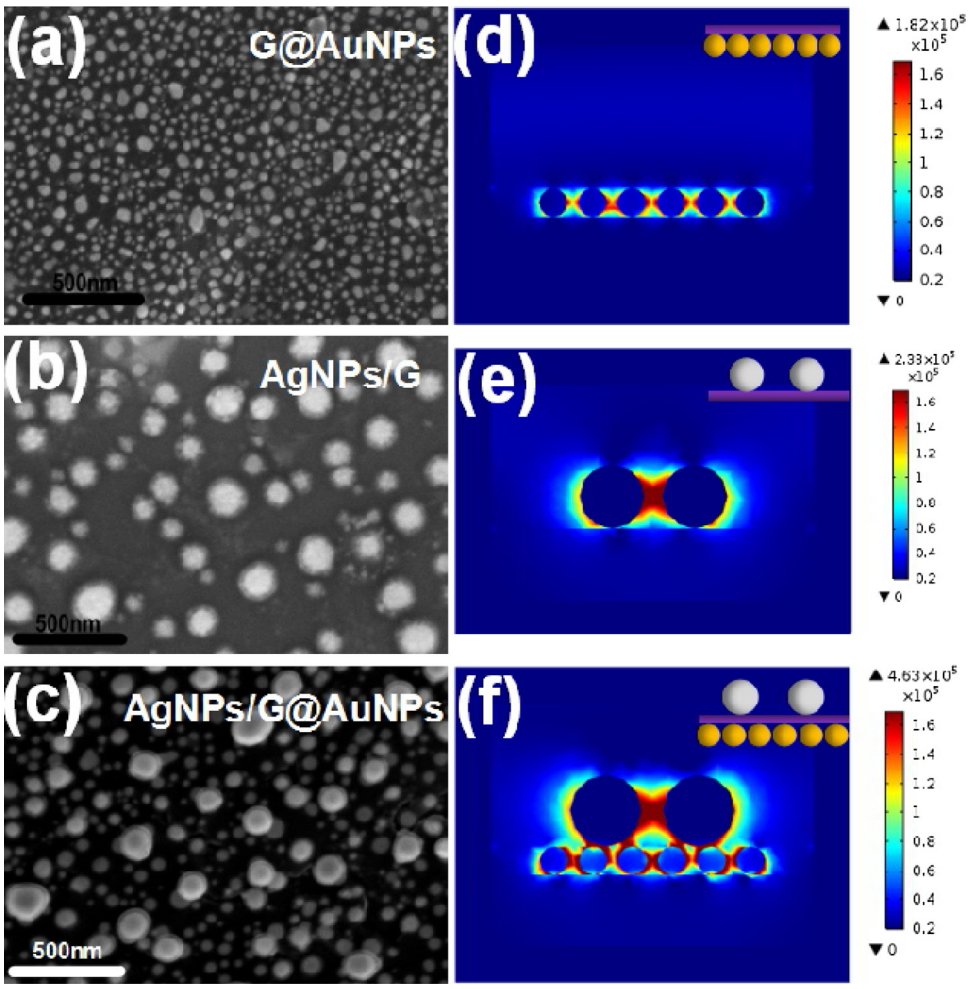

Fig. 6. SEM images of the prepared (a) graphene@AuNPs, (b) AgNPs/graphene and (c) AgNPs/graphene@AuNPs substrate, coresponding COMSOL calculation: the y-z planes of the local electric field distribution respectively on (d) graphene@AuNPs, (e) AgNPs/graphene and (f) AgNPs/graphene@AuNPs substrates.

AgNPs/graphene@AuNPs are about 1.8-3.8 times stronger than that on graphene@AuNPs and AgNPs/graphene. The peaks of CV at 914, 1175, 1619 cm^{-1} on the AgNPs/graphene@AuNPs are about 5.1–7.5 times stronger than that on graphene@AuNPs and AgNPs/graphene.

In order to better understand and further identify the perfect SERS behaviors of the AgNPs/graphene@AuNPs substrate, the local electric field properties of these substrates were respectively calculated and analyzed using commercial COMSOL software. The theoretical models were built based on the SEM results shown in Fig. 6(a)–(c). As the SEM images exhibited combining with the energy-dispersive X-ray spectroscopy in Fig. S6, we can appreciate that the diameter of the AuNPs on the graphene@AuNPs substrate is similar with that on the AgNPs/graphene@AuNPs substrate and the diameter of the AgNPs on the AgNPs/graphene (average diameter: ~90 nm) is slightly smaller than that on the AgNPs/graphene@AuNPs, which can be attributed to the temperature variation on different substrates. The absorption spectra in Fig. S7 also demonstrate this phenomenon. The diameter of AgNPs and AuNPs on the AgNPs/graphene@AuNPs substrate was respectively set as 100 and 40 nm respectively with a lateral gap of 30 and 15 nm and the vertical gap between the AgNPs and AuNPs was set as 0.68 nm according to the graphene layer. The diameter of AuNPs on the graphene@AuNPs and AgNPs on the AgNPs/graphene was respectively set as 40 and 90 nm with a lateral gap of 15 and 25 nm. Just as expected, the intensity of the local electric field on the AgNPs/graphene@AuNPs substrate in Fig. 6(f) is ~2.54 times stronger than that on the graphene@AuNPs (Fig. 6(d)) and ~1.95 times stronger than that on the AgNPs/graphene (Fig. 6(e)). What should be noted is that, besides the enhancement of lateral local electric field, the vertical local electric field is also greatly enhanced on the AgNPs/graphene@AuNPs as obviously shown in Fig. 6(f), which will contribute to the excellent SERS behavior of this proposed SERS substrate.

After that, we next further investigate the effect of the size controllability of the decorated AuNPs and AgNPs and the width of the vertical nanogaps between AuNPs and AgNPs. The corresponding SEM results of the samples based on different thickness of Au and Ag film and different layer of graphene are respectively shown in Figs. S8, S9 and S10. With the increasing the thickness (2 nm to 17 nm) of Au film, the size of AuNPs changes from smaller one to bigger one and become more sparse. Similar phenomenon is also detected for the case of AgNPs, which may be attributed to the temperature variation on different substrates introduced by the change of the thickness of the metal film. For the case of various layer of the graphene, the top (AgNPs) and bottom (AuNPs) can be distinguished by their brightness in SEM figures. In other word, the bottom AuNPs look like covered by a thin layer of silk that supports the top AgNPs, and look slightly foggy in case of existing graphene compared to that without graphene (AgNPs/0G@AuNPs) in Fig. S10(a). And the morphology of AuNPs and AgNPs on AgNPs/2G@AuNPs, AgNPs/4G@AuNPs, AgNPs/6G@AuNPs and AgNPs/8G@AuNPs respectively corresponding to Figs. S8(b), S10(b), S10(c) and S10(d) is not sensitive to the spacer-layer of graphene. The R6G molecules (10^{-5} M) is chosen as

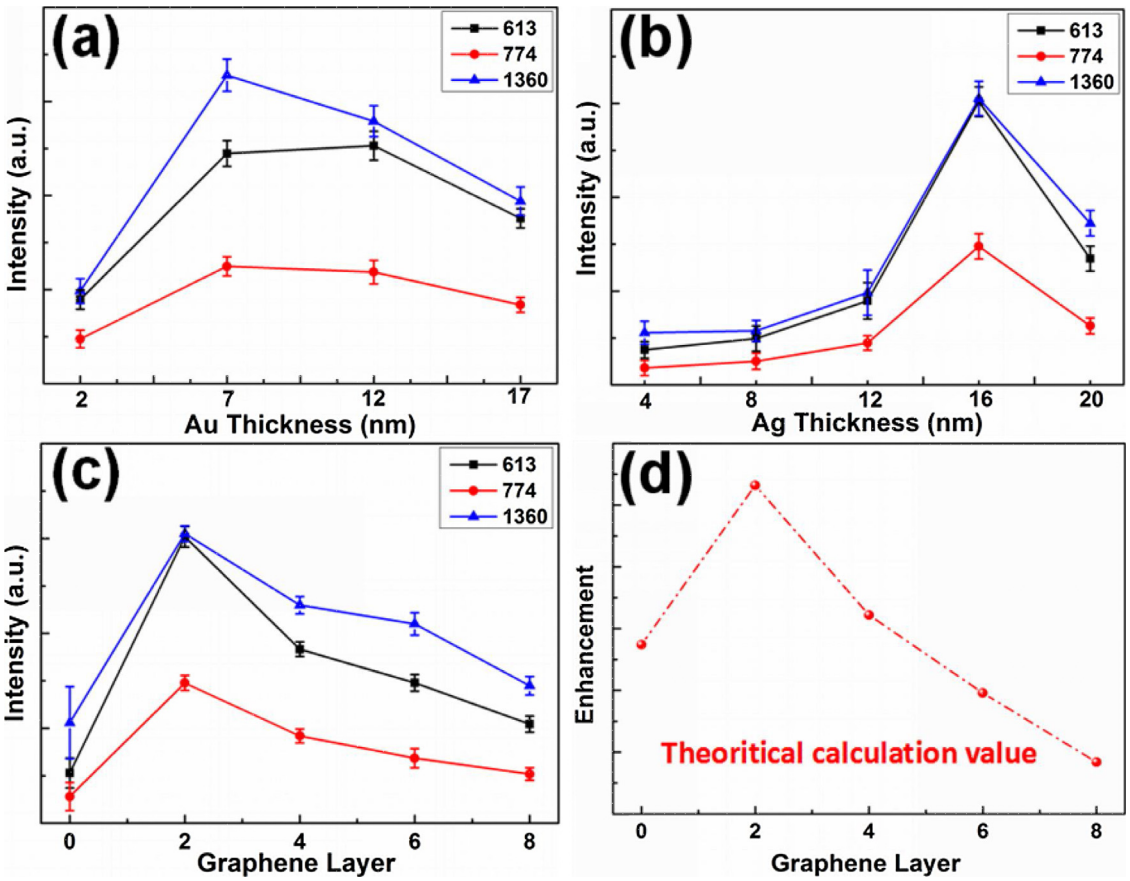

Fig. 7. The relative intensity of the peaks at 613, 774 and 1360 cm^{-1} from R6G (10^{-5} M) molecules based on the increase of thickness of (a) Au and (b) Ag film, and (c) the different layer of graphene. (d) The theoritical calculation value of the local electromagnetic field for the different layer of graphene.

the probe to estimate the SERS performance of the different substrates based on different thickness of Au and Ag film and different layer of graphene as shown in Fig. S11. The relative intensity of the peaks at 613, 774 and 1360 cm^{-1} on different substrates presented in Fig. 7(a), (b) and (c) exhibit a similar trend, where a decrease can be detected after the rise with the increase of thickness of Au and Ag film and the layer of graphene. The highest SERS intensities were obtained from the AgNPs (16 nm Ag film)/2G@AuNPs (7 nm Au film) as shown in Fig. 7(a), (b) and (c). Just as expected, the calculated enhanced intensity of the local electric field in Fig. 7(d) (extracted from Fig. S12) provides further evidence for the excellent behaviors of the AgNPs/2G@AuNPs, which is well consistent with the experimental result in Fig. 7(c) and demonstrate that the plasmon tunneling phenomenon due to the narrow gap (<0.5 nm) between AgNPs and AuNPs will result in reducing the plasmonic coupling effect and weakening the Raman signal. Therefore, monolayer graphene was not adopted in our work. Besides, the enhanced local electric field will exponentially decay with the increase of the nanogap. What should be noted is that the LSPs or hot spots, distributed not only at lateral nanogaps (AuNPs-AuNPs, AgNPs-AgNPs) but also at the tunable vertical nanogaps by graphene between AgNPs and AuNPs in our work, which can greatly enhance the Raman signal.

To research the potential possibility of AgNPs/graphene@AuNPs SERS platform applying in real samples, we carried out the SERS detection of MG, a chemical of poisonous triphenylmethane [32], in both DI and sea water. To verify that the prepared AgNPs/graphene@AuNPs can be satisfied with the actual requirements, MG was added to the DI water and prepared the solution with concentrations from 10^{-5} to 10^{-11} M. The characteristic Raman peaks of MG molecules for the concentration respectively from 10^{-5} to 10^{-11} M located at 437, 799, 912, 1170 and 1614 cm^{-1} as well as the peaks of graphene such as 2D peak can be easily detected in Fig. 8(a). And the linear fit curve in Fig. 8(b) (R^2 can reach to about 0.994) of the vibrations of MG located at 1614 cm^{-1} with error bars based on ten spectra randomly is presented, which prove the capacity of quantitative detection for the MG molecules. Thus, these aforementioned results demonstrate the proposed AgNPs/graphene@AuNPs substrate possesses virtues of ideal SERS substrate and can meet practical application. The sea water (obtained from local seafood supermarket) was chosen as solvent and was used to dilute MG molecules to the concentration of 10^{-5} M. Based on the insert in Fig. 8(c), one can see clearly that unlike that in DI water, the MG solutions in sea water is colorless and transparent just like pure water, which can be attributed to some complex components in sea water and will present a misleading for the customers. It can be seen that even diluted in sea water, the characteristic Raman peaks of MG can also be detected on AgNPs/graphene@AuNPs in Fig. 8(c). As a comparison, MG diluted in DI water (black curve in Fig. 8(c)) with 10^{-5} M also was detected and the intensity of the spectrum is a little higher than that of MG diluted in sea water, which may be introduced by the complex components such as NaCl crystal (in micro-image in Fig. 8(d)) in sea water. The high uniformity of novel SERS substrate is extremely significant for the pratical application. Therefore, the futher uniform detection of MG in sea water (10^{-8} M) on the homogeneity of the AgNPs/graphene@AuNPs substrate was carried out as presented in Fig. S13, which indicates that the uniformity of SERS signals. Therefore, the SERS spectra of MG diluted in sea water obtained from the

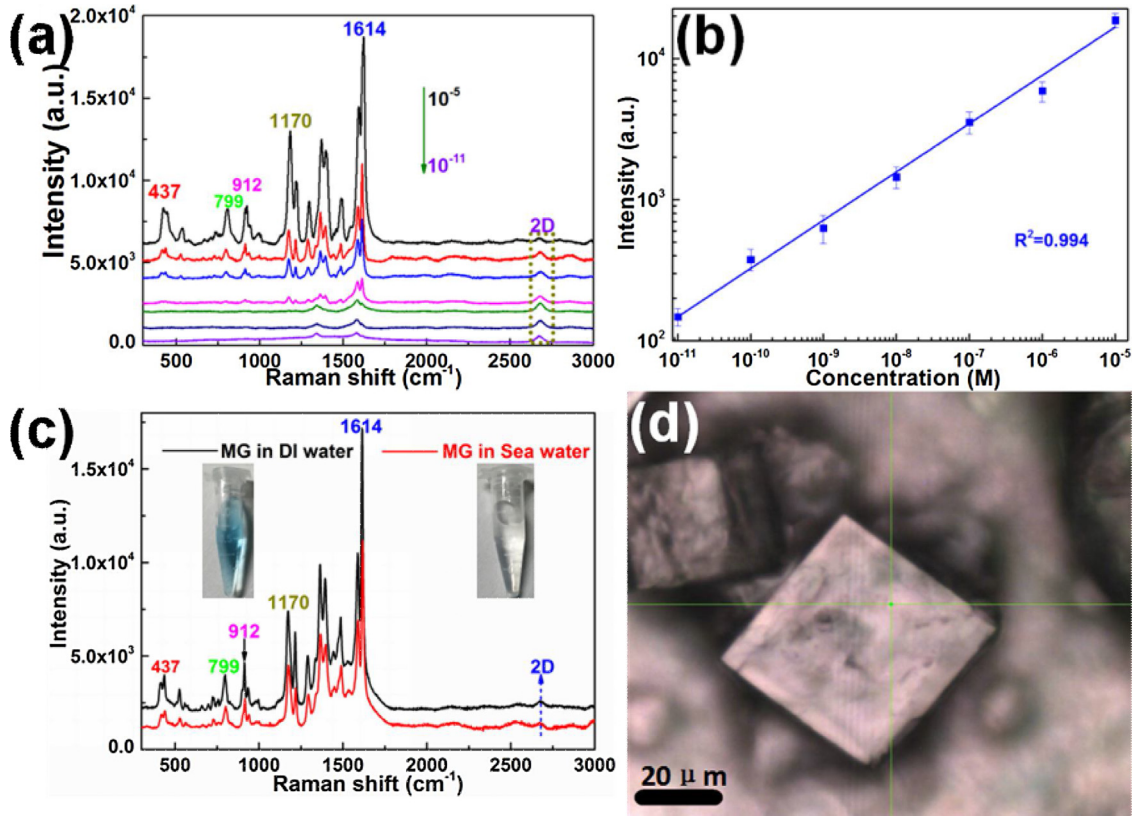

Fig. 8. (a) Raman spectra of MG in various concentrations in DI water. (b) The relative intensity of MG for the peak of 1614 cm^{-1} in DI water detected on AgNPs/graphene@AuNPs, as a function of the concentration of MG molecules. (c) Raman spectra of MG for 10^{-5} M diluted in sea water (red curve) and in DI water (black curve). Inset: the prepared MG solutions respectively in sea water and DI water. (d) The surface micrograph of AgNPs/graphene@AuNPs substrate detected by 50 × objective after MG solution (in sea water) was dry in the lab atmosphere. (For interpretation of the references to colour in this figure legend, the reader is referred to the web version of this article.)

AgNPs/graphene@AuNPs demonstrated the vast potential ability for practical application in the food safety.

4. Conclusion

In summary, AgNPs/graphene@AuNPs system with a tunable nanometer gap as SERS substrate has been prepared with a simple method. Based on the proposed AgNPs/graphene@AuNPs substrate, the perfect SERS behaviors were investigated using R6G and CV experimentally and commercial COMSOL software theoretically. In the proposed AgNPs/graphene@AuNPs substrate, the hot spots in all three dimensions can be effectively excited by the lateral and vertical nanogaps, which is much beneficial for the enhancement of the EM. The graphene not only can provide the SERS enhancement from CM, but also can act as a nanometer ruler to accurately control the size of the nanogaps by changing the layers of graphene. The contrast SERS spectra of the substrate with different nanogaps demonstrated that the optimal size of the nanogap is 0.68 nm. For practical application, the spectra of MG in DI and sea water were also collected and the detection limit was achieved (10^{-11} M) as low as the European Union's standard: 5.48 nM, which show the wide potential in food safety.

Acknowledgments

The authors are grateful for financial support from the National Natural Science Foundation of China (11474187, 11674199 and 11604040), Shandong Province Natural Science Foundation (ZR2017BA004, ZR2014FQ032, ZR2016AM19), China Postdoctoral Science Foundation (2016M600550, 2016M602716), A Project of Shandong Province Higher Educational Science and Technology Program (J15LJ01) and Excellent Young Scholars Research Fund of Shandong Normal University.

References

[1] S.C. Xu, B.Y. Man, S.Z. Jiang, J.H. Wang, J. Wei, S.D. Xu, H.P. Liu, S.B. Gao, H.L. Liu, Z.H. Li, H.S. Li, H.W. Qiu, Graphene/Cu nanoparticle hybrids ffabricated by chemical vapor deposition as surface-enhanced raman scattering substrate for llabel-free detection of adenosine, ACS Appl. Mater. Interfaces 7 (2015) 10977–10987.
[2] S.N. Chen, X. Li, Y.Y. Zhao, L.M. Chang, J.Y. Qi, Graphene oxide shell-isolated Ag nanoparticles for surface-enhanced raman scattering, Carbon 81 (2015) 767–772.
[3] B. Kiraly, S. Yang, T.J. Huang, Multifunctional porous silicon nanopillar arrays: antireflection superhydrophobicity, photoluminescence, and surface-enhanced raman scattering, Nanotechnology 24 (2013) 245704.
[4] S.Y. Lee, H. Chon, S.Y. Yoon, E.K. Lee, S.I. Chang, D.W. Lim, J.B. Choo, Fabrication of SERS-fluorescence dual modal nanoprobes and application to multiplex cancer cell imaging, Nanoscale 4 (2012) 124–129.
[5] M.L. Seol, S.J. Choi, D.J. Baek, T.J. Park, J.H. Ahn, S.Y. Lee, Y.K. Choi, A nanoforest structure for practical surface-enhanced raman scattering substrates, Nanotechnology 23 (2012) 095301.
[6] C. Zhang, S.Z. Jiang, C. Yang, C.H. Li, Y.Y. Huo, X.Y. Liu, A.H. Liu, Q. Wei, S.S. Gao, X.G. Gao, B.Y. Man, Gold@Silver bimetal Nanoparticles/pyramidal silicon 3D substrate with high reproducibility for high-Performance SERS, Sci. Rep. 6 (2016).
[7] J.A. Schuller, E.S. Barnard, W.S. Cai, Y.C. Jun, J.S. White, M.L. Brongersma, Plasmonics for extreme light concentration and manipulation, Nat. Mater. 9 (2010) 193–204.
[8] C. Yang, C. Zhang, Y.Y. Huo, S.Z. Jiang, H.W. Qiu, Y.Y. Xu, X.H. Li, B.Y. Man, Shell-Isolated Graphene@Cu nanoparticles on Graphene@Cu substrates for the application in SERS, Carbon 98 (2016) 526–533.
[9] H.G. Duan, K. Hu, Z.X. Shen, J.K.W. Yang, Direct and reliable patterning of plasmonic nanostructures with sub-10 nm gaps, ACS Nano 5 (2011) 7593–7600.

[10] T. Siegfried, L. Wang, Y. Ekinci, O.J.F. Martin, H. Sigg, Metal double layers with sub-10 nm channels, ACS Nano 8 (2014) 3700–3706.
[11] M. Melli, A. Polyakov, D. Gargas, C. Huynh, L. Scipioni, W. Bao, D.F. Ogletree, P.J. Schuck, S. Cabrini, A. Weber-Bargioni, Reaching the theoretical resonance quality factor limit in coaxial plasmonic nanoresonators fabricated by helium ion lithography, Nano Lett. 13 (2013) 2687–2691.
[12] R. Stosch, F. Yaghobian, T. Weimann, R.J.C. Brown, M.J.T. Milton, B. Güttler, Lithographical gap-size engineered nanoarrays for surface-enhanced raman probing of biomarkers, Nanotechnology 22 (2011) 105303.
[13] I. Yoon, T. Kang, W. Choi, J.B. Kim, Y.D. Yoo, S.W. Joo, Q.H. Park, H. Ihee, B.S. Kim, Single nanowire on a film as an efficient SERS-active platform, J. Am. Chem. Soc. 131 (2008) 758–762.
[14] H. Kim, M.L. Seol, D.I. Lee, J.Y. Lee, S.Y. Kang, H.B. Lee, T.J. Kang, Y.K. Choi, B.S. Kim, Single nanowire on graphene (SNOG) as an efficient, reproducible, and stable SERS-active platform, Nanoscale 8 (2016) 8878–8886.
[15] X.H. Li, X.G. Ren, Y.X. Zhang, W.C.H. Choy, B.Q. Wei, An all-Copper plasmonic sandwich system obtained through directly depositing copper NPs on a CVD grown graphene/copper film and its application in SERS, Nanoscale 7 (2015) 11291–11299.
[16] Z.Y. Zhan, L.H. Liu, W. Wang, Z.J. Cao, A. Martinelli, E. Wang, Y. Cao, J.N. Chen, A. Yurgens, J. Sun, Ultrahigh surface-enhanced Raman scattering of graphene from Au/graphene/Au sandwiched structures with subnanometer gap, Adv. Optic. Mater. 4 (2016) 2021–2027.
[17] K.J. Lee, D. Kim, B.C. Jang, D.W. Kim, B.C. Jang, D.J. Kim, H. Park, D.Y. Jung, W. Hong, T.K. Kim, Y.K. Choi, S.Y. Choi, Multilayer graphene with a rippled structure as a spacer for improving plasmonic coupling, Adv. Funct. Mater. 26 (2016) 5093–5101.
[18] Q. Xiang, X.P. Zhu, Y.Q. Chen, H.G. Duan, Surface enhanced raman scattering of gold nanoparticles supported on copper foil with graphene as a nanometer gap, Nanotechnology 27 (2016) 075201.
[19] S. Vaidya, A. Patra, A.K. Ganguli, Optical properties of Ag@TiO_2 and CdS@TiO_2 core-Shell nanostructures, Sci. Adv. Mater. 4 (2012) 631–636.
[20] G.H. Ding, S. Xie, Y. Zhu, Y. Liu, L. Wang, F. Xua, Graphene oxide wrapped Fe_3O_4@Au nanohybrid as SERS substrate for aromatic dye detection, Sens. Actuators B 221 (2015) 1084–1093.
[21] J.F. Li, Y.F. Huang, Y. Ding, Z.L. Yang, S.B. Li, X.S. Zhou, F.R. Fan, W. Zhang, Z.Y. Zhou, D.Y. Wu, B. Ren, Z.L. Wang, Z.Q. Tian, Shell-isolated nanoparticle-enhanced raman spectroscopy, Nature 464 (2010) 392–395.
[22] X.Y. Zhang, J. Zhao, A.V. Whitney, J.W. Elam, R.P. Van Duyne, Ultrastable substrates for surface-enhanced raman spectroscopy: Al_2O_3 overlayers fabricated by atomic layer deposition yield improved anthrax biomarker detection, J. Am. Chem. Soc. 128 (2006) 10304–10309.
[23] L.W. Ma, Y. Huang, M.J. Hou, Z. Xie, Z.J. Zhang, Silver nanorods wrapped with ultrathin Al_2O_3 layers exhibiting excellent SERS sensitivity and outstanding SERS stability, Sci. Rep. 5 (2015) 12890.
[24] C. Zhang, B.Y. Man, C. Yang, S.Z. Jiang, M. Liu, C.S. Chen, S.C. Xu, Z.C. Sun, X.G. Gao, X.J. Chen, Facile synthesis of graphene on dielectric surfaces using a two-temperature reactor CVD system, Nanotechnology 24 (2013) 395603.
[25] C.H. Zhang, S.L. Zhao, C.H. Jin, A.L. Koh, Y. Zhou, W.G. Xu, Q.C. Li, Q.H. Xiong, H.L. Peng, Z.F. Liu, Direct growth of large-area graphene and boron nitride heterostructures by a Co-segregation method, Nat. Commun. 6 (2015) 6519.
[26] J.J. Li, H.Q. An, J. Zhu, J. Zhao, Detecting glucose by using the Raman scattering of oxidized ascorbic acid: the effect of graphene oxide–gold nanorod hybrid, Sens. Actuators B 235 (2016) 663–669.
[27] J. Du, J.Y. Li, N. Kang, L. Li, H.L. Peng, Z.F. Liu, H.Q. Xu, Probe of local impurity states by Bend resistance measurement in graphene cross junctions, Nanotechnology 27 (2016) 245204.
[28] C. Zhang, B.Y. Man, C. Yang, S.Z. Jiang, M. Liu, C.S. Chen, S.C. Xu, X.G. Gao, Z.C. Sun, Direct formation of graphene-carbon nanotubes hybrid on SiO_2 substrate via chemical vapor deposition, Sci. Adv. Mater. 6 (2014) 399–404.
[29] C. Zhang, S.Z. Jiang, Y.Y. Huo, A.H. Liu, S.C. Xu, X.Y. Liu, Z.C. Sun, Y.Y. Xu, Z. Li, B.Y. Man, SERS detection of R6G based on a novel graphene oxide/silver nanoparticles/silicon pyramid arrays structure, Opt. Express 23 (2015) 24811–24821.
[30] C.H. Li, C. Yang, S.C. Xu, C. Zhang, Z. Li, X.Y. Liu, S.Z. Jiang, Y.Y. Huo, A.H. Liu, B.Y. Man, Ag_2O@Ag core-shell structure on PMMA as low-cost and ultra-sensitive flexible surface-enhanced raman scattering substrate, J. Alloy. Compd. 695 (2017) 1677–1684.
[31] M.J. Natan, Concluding remarks surface enhanced Raman scattering, Faraday Dis. 132 (2006) 321–328.
[32] A.R. Shalaby, W.H. Emam, M.M. Anwar, Mini-column assay for rapid detection of malachite green in fish, Food Chem. (2017).

Biographies

Chao Zhang is a researcher in School of Physics and Electronics, Shandong Normal University, People's Republic of China. He has received Ph.D. degree from Shandong Normal University in 2016. His research interests are the synthesis and applications of nanomaterials, plasmonics, SERS sensors.

Chong Hui Li is studying as a doctor in School of Physics and Electronics, Shandong Normal University, People's Republic of China. His researcher interest is the functionalization of two-dimension materials.

Jing Yu is a researcher in School of Physics and Electronics, Shandong Normal University, People's Republic of China. He has received Ph.D. degree from University of Science and Technology of China. He focuses the research on the nanomaterials and plasmonics,

Shou Zhen Jiang is a researcher in School of Physics and Electronics, Shandong Normal University, People's Republic of China. He obtained his Ph.D. degree from Shandong University in 2007. His research interests center on the optical properties of two-dimension materials.

Shi Cai Xu is a researcher in College of Physics and Electronic Information, Dezhou University, China. He received Ph.D. degree from the School of Physics and Electronics, Shandong Normal University, People's Republic of China in 2014. Now he researches on the region of graphene fabrication and DNA nanotechnology.

Cheng Yang is a researcher in School of Physics and Electronics, Shandong Normal University, People's Republic of China. He obtained his Ph.D. degree from Sungkyunkwan University. His research area is the surface plasma.

Yan Jun Liu is a researcher in Southern University of Science and Technology, People's Republic of China. He now researches on the preparation and application of MoS2 and WS2.Xingguo Gao is a researcher in School of Science, Qilu University of Technology, People's Republic of China. He now mainly simulates the optical properties of two-dimension materials.

Xingguo Gao is a researcher in School of Science, Qilu University of Technology, People's Republic of China. He now mainly simulates the optical properties of two-dimension materials.

Ai Hua Liu is a professor in School of Physics and Electronics, Shandong Normal University, People's Republic of China. She now researches on the preparation of two-dimension materials and applications in optoelectronic device.

Bao Yuan Man is a professor in School of Physics and Electronics, Shandong Normal University, People's Republic of China. His research interest is centered on the preparation and application of Dirac materials.